Neurochemistry International 128 (2019) 115–126

Contents lists available at ScienceDirect

Neurochemistry International

journal homepage: www.elsevier.com/locate/neuint

Thymoquinone prevents neurodegeneration against MPTP *in vivo* and modulates α-synuclein aggregation *in vitro*

Mustafa T. Ardah[1], Madiha Mohieldin Merghani[1], M. Emdadul Haque[*]

Department of Biochemistry, College of Medicine and Health Sciences, United Arab Emirates University, PO Box, 17666, Al Ain, United Arab Emirates

ARTICLE INFO

Keywords:
Thymoquinone
Neurodegeneration
Neurotoxicity
Parkinson's disease
α-synuclein
MPTP

ABSTRACT

Parkinson's disease (PD) is a common neurodegenerative disease characterized by progressive dopaminergic neurodegeneration with a concomitant increase in oxidative stress and neuroinflammation in the substantia nigra pars compacta (SNc). Recent studies have focused on targeting neuroinflammation and oxidative stress to effectively treat PD. The present study evaluated the neuroprotective effect of thymoquinone (TQ) against 1-methyl-4-phenyl 1,2,3,6 tetrahydropyridine (MPTP)-induced oxidative stress and neuroinflammation in a PD mouse model. TQ (10 mg/kg body weight [*b. wt.*]) was administered for 1 week prior to MPTP (25 mg/kg b. *wt.*). MPTP administration caused oxidative stress as evidenced by decreased activities of superoxide dismutase and catalase, a depletion of reduced glutathione, and a concomitant rise in malondialdehyde. It also significantly increased pro-inflammatory cytokines and elevated inflammatory mediators such as cyclooxygenase-2 (COX-2) and inducible nitric oxide synthase (iNOS) in the striatum. Immunohistochemical analysis revealed dopamine neuron loss in the SNc and decreased dopamine transporters in the striatum following MPTP administration; however, these were rescued by TQ treatment. TQ treatment further restored antioxidant enzymes, prevented glutathione depletion, inhibited lipid peroxidation, and attenuated pro-inflammatory cytokines. TQ also decreased the raised levels of inflammatory mediators, such as COX-2 and iNOS. Therefore, TQ is thought to protect against MPTP-induced PD and the observed neuroprotective effects are attributed to its potent antioxidant and anti-inflammatory properties. Moreover, the *in vitro* analysis found that TQ significantly inhibited α-synuclein aggregation and prevented cell death induced by pre-formed fibrils. Thus, TQ not only scavenges the MPTP-induced toxicity but also prevents α-synuclein-fibril formation and its associated toxicity.

1. Introduction

Parkinson's disease (PD) is an age-related neurodegenerative disease that is characterized by selective nigrostriatal dopaminergic neurodegeneration and the presence of intraneuronal cytoplasmic inclusions known as Lewy bodies, consisting primarily of α-synuclein (α-syn). Globally, it is estimated that approximately 1% of the population over 60 years of age is affected; however, as the international life expectancy is steadily rising, we anticipate that this number will increase in the coming years. Although the exact mechanisms of the selective loss of dopamine (DA) neurons in the substantia nigra pars compacta (SNc) are not fully understood, excessive free-radical formation due to mitochondrial dysfunction, impaired ubiquitin proteasome function, inflammation, autophagy, and aberrant α-syn aggregation are believed to be involved in the progression of PD (Beal, 2003; Hald and Laotharius, 2005; Casey et al., 2012; Rocha et al., 2017). Current literature demonstrates that genetic and environmental risk factors are implicated in the etiology of PD; exposure to environmental toxicants such as rotenone, paraquat, and 1-methyl-4-phenyl 1,2,3,6 tetrahydropyridine (MPTP) are thought to increase the risk of developing PD (Sanders et al., 2013; He et al., 2015; Tinakoua et al., 2015).

Among the various dopaminergic neurotoxins, MPTP has been highlighted due to its ability to produce clinical features of PD in humans and monkeys. MPTP is highly lipophilic and readily crosses the blood brain barrier and enters into astrocytes. In astrocytes, MPTP is oxidized into its toxic metabolite 1-methyl-4-phenylpyridinium (MPP +), which causes the death of Dopamine (DA) neurons and results in parkinsonism in experimental animal models. Therefore, MPTP has

Abbreviations: DAB, 3,3′-diaminobenzidine; GSH, glutathione; MDA, malondialdehyde; MPTP, 1-methyl-4-phenyl 1,2,3,6 tetrahydropyridine; PD, Parkinson's disease; SOD, superoxide dismutase; α-syn, α-synuclein; TQ, thymoquinone; Th-S, thioflavin-S

* Corresponding author.
E-mail address: ehaque@uaeu.ac.ae (M.E. Haque).
[1] These authors contributed equally to this work.

https://doi.org/10.1016/j.neuint.2019.04.014
Received 29 January 2019; Received in revised form 1 April 2019; Accepted 23 April 2019
Available online 24 April 2019

been used to develop animal models of PD to test new therapies, which are valuable pharmacological tools for studying the mechanisms of oxidative stress and inflammation-induced dopaminergic damage and evaluating novel pharmacotherapeutic agents for PD.

Furthermore, α-syn can undergo conformational changes, which promotes its self-assembly and aggregation. α-syn aggregation proceeds through the formation of oligomers (early aggregates), which ultimately convert into well-ordered fibrils (late aggregates) (Uversky et al., 2001). It has been reported that the early aggregate oligomers are the pathogenic species causing neurodegeneration and neuronal cell death, rather than the mature amyloid fibrils (El-Agnaf et al., 2003; Conway et al., 2000; Winner et al., 2011). Recent studies have demonstrated that insertion of aggregated α-syn (pre-formed fibrils) into the striatum of mouse brains propagate from the injection site to other brain regions that innervate the striatum by a prion-like mechanism, while also inducing DA neuronal death (Luk et al., 2012a, 2012b). Thus, the role of α-syn is of importance, not only because of its pathogenic role in sporadic and familial PD, but also because it may elucidate the mechanisms underlying the pathogenesis of PD. Additionally, the inhibition of the aberrantly formed α-syn and its propagation can be used as a model to identify potential drugs for PD.

Thymoquinone (TQ) is the most abundant component found in the plant *Nigella sativa*, also known as black seed or black cumin (AbuKhader, 2013). Black seed oil extracts have been used in traditional medicine in the Middle East and India (Hamdy and Taha, 2009). Most importantly, Prophet Muhammad (SWS) once stated that black cumin or habbatus sauda (the black seed of *Nigella sativa*) can heal many diseases (Ahmad et al., 2013). TQ has low toxicity (LD50, 2.5 g/kg) and is generally well tolerated when administered subchronically, up to a dose of 90 mg/kg/day for 90 days (Elmaci and Altinoz, 2016). Numerous studies have demonstrated that TQ has potent anti-inflammatory and antioxidant activities (Hamdy and Taha, 2009; Taka et al., 2015; Gore et al., 2016). Moreover, TQ has been shown to decrease the level of malondialdehyde (MDA), a marker of oxidative stress, and prevent dopaminergic neurodegeneration in the 6-hydroxydopamine (6-OHDA)-induced hemi-Parkinson rat model, which suggests its antioxidant role (Sedaghat et al., 2014). MPP + or rotenone-induced toxicity in primary dopaminergic neuronal cultures isolated from the mouse midbrain can be ameliorated with TQ treatment (Radad et al., 2009, 2015). TQ is not only beneficial in neurotoxic models, but also protects dopaminergic neurons against leucine-rich repeat kinase 2-induced toxicity in a genetic model of PD using drosophila (Angeles et al., 2016). Additionally, TQ protected rat cultured hippocampal neurons and human induced pluripotent stem cell-derived neurons against α-syn (α-syn-induced synapse damage) (Alhebshi et al., 2014); however, the exact biochemical mechanism of the neuroprotective action of TQ in a well characterized *in vivo* PD model has not yet been demonstrated.

The aim of the present study was to investigate the role of TQ in MPTP-induced PD with an *in vivo* mouse model that mimics most of the pathological features of human PD. The MPTP injected mouse, which is widely used as a preclinical model to test the potential efficacy of drugs, has been shown to develop a PD-like phenotype characterized by loss of dopaminergic neurons and activation of neuroinflammation. We also investigated the modulating effects of TQ on α-syn aggregation, which are critical in dopaminergic neurodegeneration in sporadic PD.

2. Materials and methods

2.1. Experimental animals

Male C57BL/6c mice aged 2–3 months (25–30 g body weight) bred in the animal research facility of the College of Medicine and Health Sciences (United Arab Emirates University, UAE) were used in the present study. A maximum of two mice were housed per cage and were acclimatized to the laboratory conditions for 1 week prior to the start of the experiment. The animals were housed under standard laboratory conditions of light and dark cycle. The animals had access to commercially available rodent food and water *ad libitum*. All the experiments were carried out between 09:00 and 17:00 h. The experimental protocol for animal experimentation was approved by the Animal Ethics Committee of the College of Medicine and Health Sciences at United Arab Emirates University.

2.2. Experimental design

Mice were intraperitoneally (i.p.) injected with MPTP once daily for 5 consecutive days (25 mg/kg body weight [*b. wt.*] measured as a free base; MPTP-HCL; Sigma-Aldrich, St. Louis, MO, USA). MPTP was first dissolved in normal saline to obtain the desired concentration for the injection. The regimen used in the current study for the induction of parkinsonism in the mice was adopted from a previous report (Haque et al., 2012). To assess the neuroprotective efficacy of TQ, it was first dissolved in a minimum volume of absolute ethanol and then diluted in olive oil and injected i.p. at a dose of 10 mg/kg b. *wt.* once daily for 1 week, 60 min prior to each dose of MPTP administration. The dose of TQ was selected based on a dose-dependent study (5, 10, 20 mg/kg/b. *wt.*) performed in a different set of experiments and did not show any *in vivo* toxicity (unpublished data). The control group received an equal amount of vehicle only. The mice were divided into four experimental groups, each containing six to eight mice. The experimental groups were: Group I: Vehicle and saline injected control (V + Sal); Group II: Vehicle-treated and MPTP-injected (V + MPTP); Group III: TQ-treated and MPTP-injected (TQ + MPTP); and Group IV: TQ-treated and saline injected (TQ + Sal).

2.3. Tissue preparation for biochemical analysis

At the end of the experiments, the animals were anaesthetized with pentobarbital (40 mg/kg b. *wt.*) and cardiac perfusion was performed using 0.01 M phosphate-buffered saline (PBS; pH 7.4) to wash out the blood. The brains were quickly removed and placed on an ice-plate and the striatal region was dissected and immediately frozen in liquid nitrogen for further biochemical assay analysis.

2.4. Biochemical analysis

KCl buffer (Tris-HCl 10 mM, NaCl 140 mM, KCl 300 mM, ethylenediaminetetraacetic acid [EDTA] 1 mM, Triton X-100 0.5%, 1X PPI) was used to homogenize the striatum. The homogenates were then centrifuged at 14 000 g at 4 °C for 20 min. The total protein in the cleared supernatant was then estimated using the bicinchoninic acid (BCA) assay and stored at −80 °C for further analysis.

2.5. Estimation of lipid peroxidation

The amount of lipid peroxidation in the samples was determined using the MDA assay kit (Northwest Life Science Specialties LLC, Vancouver, WA, USA). The kit was used as per manufacturer's instructions and as previously described (Ojha et al., 2015). The samples (1 mg total protein) or standards (125 µl) were incubated in the presence of acid reagent (125 µl) and thiobarbituric acid (125 µl) and was vortexed vigorously. Samples were incubated for 60 min at 60 °C and then centrifuged at 10 000 g for 2–3 min. The reaction mixture was transferred to a 96-well clear plate (150 µl/well in duplicate) and recorded the spectra at 532 nm. The results were expressed as µM MDA/mg protein.

2.6. Reduced glutathione (GSH) estimation

A GSH kit (Sigma Cat #38185; Sigma-Aldrich) was used for the estimation of GSH according to the manufacturer's instructions and as

previously described (Ojha et al., 2015). Briefly, the GSH standard was prepared by mixing 100 µl of 200 µmol/l GSH standard solution and 300 µl of 0.5% 5-sulfosalicylic acid (SSA) solution in a microfuge tube to prepare a 50 µmol/GSH standard solution. This standard solution was used to prepare the following GSH standard solutions by serial dilution using 0.5% SSA solution: 50.0, 25.0, 12.5, 6.25, 3.13, 1.57, and 0 µmol/l. Then, 40 µl of GSH standard solution and samples were added to a 96-well plate in triplicate. The absorbance was measured at 405 nm using a plate reader and the results were expressed as µM GSH/mg protein.

2.7. Antioxidant enzyme activity estimation

The superoxide dismutase (SOD) and catalase (CAT) were determined using kits purchased from Cayman Chemicals Company (Ann Arbor, MI, USA). The estimation was carried out following the manufacturer's instructions and as previously described (Ojha et al., 2015). Briefly, the formaldehyde standards were prepared as 0, 5, 15, 30, 45, 60, and 75 µM. Twenty microliters of the prepared standards and 30 µl of methanol were then added to each well in the plate. The reaction was initiated by adding 20 µl of diluted hydrogen peroxide. After 20 min of incubation at room temperature (RT), 30 µl of potassium hydroxide was added to each well to terminate the reaction, followed by 30 µl of catalase purpald, Chromogen (Cayman Chemicals Company). Before reading the absorbance at 540 nm, 10 µl of catalase potassium periodate was added to each well. For SOD measurements, sample or standard (10 µl each) were added to a well of a 96-well plate. Xanthine oxidase (20 µl) was added to each well to initiate the reaction. The plate was shaken for a few seconds and then covered with a plate cover and incubated for 30 min at RT. Absorbance was read at 450 nm by using a microplate reader. The CAT activity was expressed as nmol/min/mg protein and the SOD activity was expressed as U/mg protein.

2.8. Pro-inflammatory cytokine estimation

To estimate interleukin (IL)-1β, IL-6, and tumor necrosis factor-α (TNF-α) levels in the samples, commercially available kits were purchased from R&D Systems (Minneapolis, MN, USA). Briefly, the diluted capture antibody (100 µl) was used to coat the 96-well plate overnight at RT. After washing with wash buffer (0.05% Tween 20 in 0.01 M PBS, pH 7.4), the samples were blocked with 300 µl reagent diluent (1% bovine serum albumin in PBS) for 1 h. Thereafter, 100 µl of the sample or standard was added and incubated for 2 h. After washing, the detection antibody (100 µl) was added and then incubated for 2 h at RT. A working solution (1:200) of streptavidin horseradish peroxidase (100 µl) was then added and incubated for 20 min, followed by a substrate solution (100 µl) and incubating for another 20 min. Stop solution (2 N H_2SO_4; 50 µl) was added and the plate was gently tapped to ensure proper mixing. Optical density of each well was read immediately at 450 nm using a microplate reader. The results were expressed as pg/mg protein.

2.9. Immunostaining and assessment of tyrosine hydroxylase (TH) in the SNc and DA transporters in the striatum

Mouse brains were collected as described in Section 2.3 and sectioned for TH and DA transporter (DAT) staining. For the evaluation of TH neurons, we employed an optical fractionator using Stereo Investigator (version 2017; MBF Bioscience, Williston, VT, USA), as previously described (Haque et al., 2012). In brief, 40 µm brain sections were examined within the rostral and caudal limits of the SNc (−2.54 to −3.88 mm of bregma). For each brain, seven coronal sections were examined. Serial sections of the mouse brain covering TH neurons in the SNc were washed twice with 0.01 M PBS (pH 7.4) and then incubated with a blocking reagent (10% normal goat serum in PBS 0.3% Triton-X 100) for 1 h. Further, the sections were incubated with the primary polyclonal rabbit antibody against TH (1:1000) overnight at 4 °C and then with a secondary antibody. Immunoreactivity of the antibodies was visualized using the avidin-biotin complex peroxidase reaction of 3,3′-diaminobenzidine (DAB). After immunoblotting, mounting, defatting, and cover slipping, the thickness of the sections was measured with a z-axis microcreator according to the manufacturer's instructions. Sections were analyzed using a 63X lens. The total number of TH positive neurons was determined using the optical fractionator and presented in a graph.

The loss of striatal fibers was evaluated by measuring the optical density of dopaminergic fibers in the striatum (adjacent to 0.3 mm of bregma) using Image J software (NIH, Bethesda, MD, USA). Striatum sections were washed twice with 0.01 M PBS (pH 7.4) and then incubated with a blocking reagent (10% normal goat serum in PBS 0.3% Triton-X 100) for 1 h. Further, the sections were incubated with a primary polyclonal rat antibody against DAT (1:1000) overnight at 4 °C and then with a secondary antibody. Immunoreactivity of the antibodies was visualized using the avidin-biotin complex peroxidase reaction of DAB. The optical density of the DAT at three different fields of each section (three sections/mouse) with an equal area within the striatum was measured for each mouse. The averages of the three areas was calculated and represented as a percentage with reference to the control. The optical density of the overlying cortex was taken as a background measure and subtracted from the value generated from the striatum. TH positive neurons and optical density of the DAT were estimated by an investigator blind to the experimental groups.

2.10. Western blot analysis of cyclooxygenase-2 (COX-2) and inducible nitric oxide synthase (iNOS)

The striatum tissue lysate used for the biochemical assays was also used to detect COX-2 and iNOS levels in the samples. In total, 20 µg of each sample was loaded in 15% sodium dodecyl sulfate (SDS)-polyacrylamide gel (PAGE) and electrophoresed; proteins were then transferred onto a polyvinylidene fluoride membrane and incubated overnight at 4 °C with a specific primary rabbit polyclonal antibody against COX-2 (1:1000) and iNOS (1:500) followed by a horseradish peroxidase-conjugated secondary antibody. The protein recognized by the antibody was visualized using a West Pico Chemiluminescent Kit (Thermo Fisher Scientific, Waltham, MA, USA). The blots were stripped and re-probed for β-actin (1:5000; monoclonal mouse; Millipore, Burlington, MA, USA), which was used as a loading control. The intensity of the bands was measured by densitometry and quantified using Image J software.

2.11. Expression and purification of recombinant human α-syn

The expression vector pT7-7 wt-α-syn (pT7-7 wt-α-syn was a gift from Hilal Lashuel, Addgene plasmid #36046) (Paleologou et al., 2008) was transformed with *E. coli* strain BL21 DE3 cells, and expression was induced by the addition of isopropyl D-thiogalactopyranoside. Cells were harvested, resuspended in a non-denatured lysis buffer (PBS containing 5 mM EDTA and 0.02% sodium azide), and homogenized using a glass homogenizer, followed by sonication for 10 min. The cell resuspension was then boiled for 10 min and cooled on ice for 30 min. Next, the cell lysate was centrifuged at 1500 × *g* for 20 min, the supernatant was dialyzed against gel filtration buffer (10 mM Tris pH 7.6, 50 mM NaCl, 1 mM EDTA, 1 mM phenylmethylsulfonyl fluoride), and the lysate was filtered using 0.22 µm filters and concentrated (2–4 ml/l of cell culture) using protein concentration columns (7K MWCO). The concentrated lysate was injected into gel filtration columns (Superdex 200) and the fractions were collected and examined by SDS gel. Selected fractions were then pooled, and the concentration was estimated using a BCA assay.

2.12. Aggregation of α-syn in vitro

The aggregation of α-syn with or without the TQ compound was carried out as previously described (Ardah et al., 2014a). Briefly, TQ stock solutions (10 mM) were prepared in absolute ethanol. α-syn samples in PBS were aged alone or in the presence of TQ at various molar ratios (TQ: α-syn molar ratios of 4:1, 2:1, and 1:1) while the final concentration of α-syn was 25 μM. The samples were incubated at 37 °C for 9 days with continuous shaking at 800 rpm in a Thermomixer (Eppendorf, Hamburg, Germany). Thioflavin-S (Th-S) binding assay was performed at each time point.

2.13. Th-S assay

A Th-S binding assay was used in the present study to monitor the fibril formation of the α-syn protein. Th-S is a fluorescent dye that interacts with fibrils containing a β-sheet structure that exhibits enhanced fluorescence upon binding to amyloid fibrils and is commonly used to monitor amyloid fibril formation. In the present study, we used a Th-S assay to monitor the effect of TQ on α-syn aggregation, and TQ inhibition was calculated using Th-S fluorescent emission maximum shifted to 486 nm. From each sample, 10 μl was added to 40 μl of Th-S (final concentration is 5 μM of α-syn and 20 μM of Th-S), using fresh samples obtained daily. Fluorescence (450/486 excitation and emission) was then measured by using a 384-well, black micro-well plate (Nunc, Roskilde, Denmark) using a microplate reader (Victor X3 2030; PerkinElmer, Waltham, MA, USA).

2.14. Transmission electron microscopy

α-syn aged alone or in the presence of TQ was incubated 9 days. Next, 5 μl quantities from each reaction were added to 400 mesh copper grids (Agar Scientific, Essex, UK), as previously described (Ardah et al., 2014a, 2014b). The samples were then fixed by adding 5 μl of 0.5% glutaraldehyde, and then stained with 2% uranyl acetate. Images were viewed using a Philips CM10 transmission electron microscope (Philips Electron Optics, Eindhoven, The Netherlands).

2.15. Seeding polymerization assay

The seeding assay was conducted as previously described (Ardah et al., 2014a, 2014b). Briefly, α-syn fibrils were fragmented by sonication to obtain short fibrils (seeds). In total, 2 μM of seeds were added to 100 μM of monomeric α-syn and incubated in the presence or absence of 10 μM or 50 μM of TQ at 37 °C for 48 h with continuous shaking. The fibril formation in α-syn samples was monitored using the Th-S binding assay as described in Section 2.13.

2.16. α-syn disaggregation assay

As described in Section 2.12, α-syn was aggregated at a concentration of 25 μM. The preformed α-syn aggregates were incubated alone or with TQ at molar ratios of TQ:α-syn = 6:1, 4:1, and 1:1. The samples of α-syn and TQ were then incubated for 48 h at 37 °C with continuous mixing at 800 rpm. The fibril content was measured using the Th-S assay at regular time points.

2.17. Culture of SH-SY5Y human neuroblastoma cells

SH-SY5Y human neuroblastoma cells were cultured in Dulbecco's Modified Eagle Medium (MEM): Nutrient Mixture F-12 (1:1) (Thermo Fisher Scientific), containing 15% fetal bovine serum and 1% penicillin-streptomycin (100 U/ml penicillin, 100 mg/ml streptomycin). The cells were maintained at 37 °C in a humidified incubator with 5% CO_2/95% air (Ardah et al., 2014a).

2.18. Cell cytotoxicity (MTT) assay

SH-SY5Y cells suspended in Dulbecco's MEM F-12 (1:1) medium were plated at a density of 10 000 cells (200 μl/well) in a 96-well plate. After 24 h, the medium was replaced with 200 μl of Opti-MEM (Thermo Fisher Scientific) serum-free medium containing α-syn aged with or without TQ at the molar ratios of α-syn:TQ = 1:4, 1:2, and 1:1. Cells were then incubated at 37 °C in 5% CO_2 for 48 h. In total, 20 μl of MTT (6 mg/ml) in PBS was added to each well and the plate was re-incubated at 37 °C for 4 h. The MTT-containing medium was removed carefully, and 100 μl of lysis buffer (15% SDS, 50% N,N-dimethylformamide; pH 4.7) was added in each well of the plate. The plate was incubated overnight at 37 °C. Absorbance values at 590 nm were recorded by a microplate reader (PerkinElmer, Waltham, MA, USA).

2.19. Silver ($AgNO_3$) staining

For silver staining, gels were fixed with 50 ml of 50% ethanol containing 10% acetic acid for 30 min, and then incubated for 15 min with 15% ethanol, followed by washing three times (5 min each) with deionized water. Next, the gels were sensitized by incubating with 0.02% (w/v) sodium thiosulfate ($Na_2S_2O_3$) for 90 s, followed by washing three times with deionized water. The washed gels were stained with 0.2% (w/v) $AgNO_3$ for 25 min, then developed with 6% (w/v) $NaCO_3$ containing 50 μl of 37% formaldehyde and 2 ml of 0.02% $Na_2S_2O_3$ until bands appeared clearly. The silver staining was stopped with 6% acetic acid.

2.20. Proteinase K (PK) digestion

Aggregated α-syn (25 μM), alone or in the presence of TQ at a molar ratio 1:1, was subjected to PK digestion (2.5 μg/ml) by incubation for 15 min at 37 °C with PK (Sigma-Aldrich) (Ardah, 2014a). To stop the digestion reaction, 2X sample loading buffer (250 mM Tris-HCl, pH 6.8, 30% glycerol, 0.02% bromophenol blue, 8% SDS, 5% beta-mercaptoethanol) was added, followed by 10 min of heating at 95 °C. The samples were then separated using 15% SDS-PAGE gels, followed by silver staining.

2.21. Protein estimation

The protein content was estimated using the Pierce BCA protein assay kit (Thermo Fisher Scientific), following the manufacturer's instructions.

2.22. Statistical analyses

The data were expressed as the mean value ± standard error of the mean. The data for all studies were analyzed using one-way analyses of variance (ANOVA) followed by Tukey's test to calculate the statistical significance between various groups using GraphPad InStat software (GraphPad Software Inc., La Jolla, CA, USA). In all the tests, the criterion for any statistically significant difference was set at ***, $p < 0.001$; **, $p < 0.01$; *, $p < 0.05$.

3. Results

3.1. TQ prevents MPTP-induced dopaminergic neurodegeneration in the SNc and DA transporters in the striatum

We evaluated the neuroprotective efficacy of TQ by assessing TH-positive DA neurons in the SNc and the optical density of striatal DA fibers. MPTP administration caused a significant loss of DA neurons in the SNc and decrease of striatal DA fibers in the brains of experimental mice when compared to vehicle-injected control mice. However,

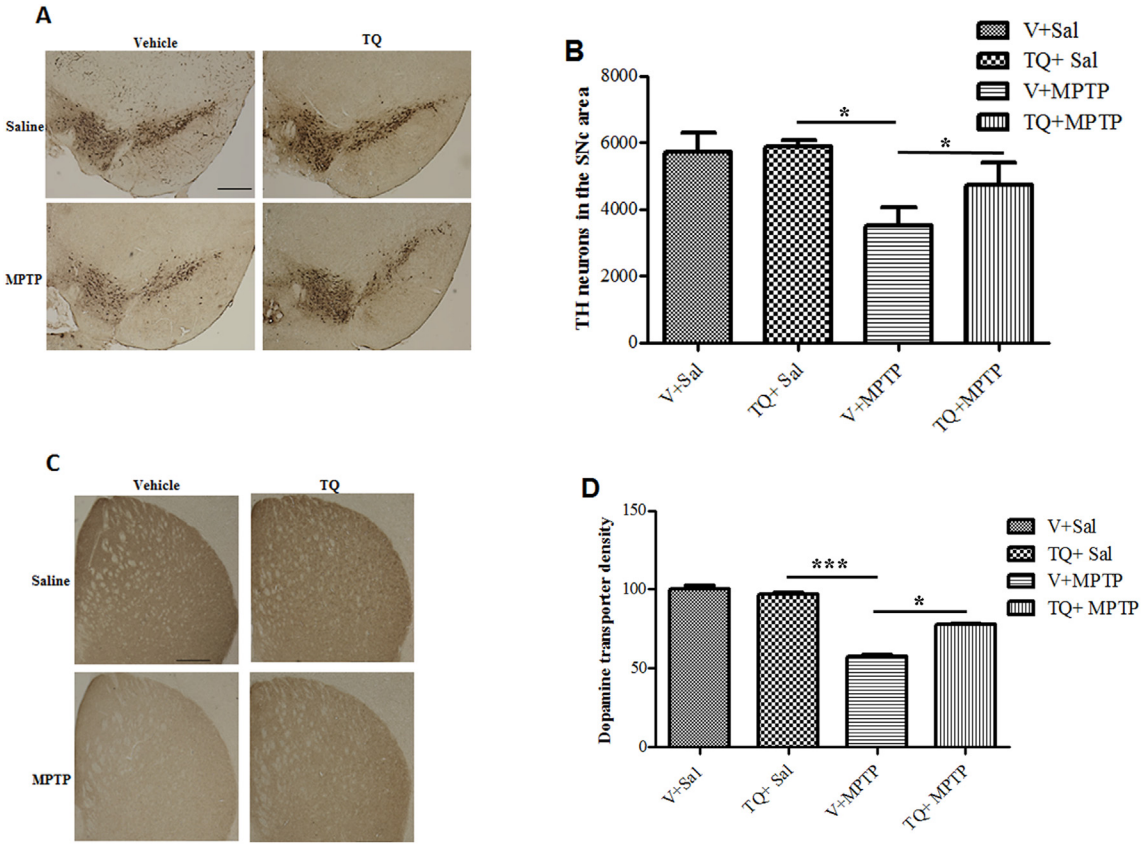

Fig. 1. Immunostaining of tyrosine hydroxylase positive (TH^+) neurons to quantify the number of dopamine (DA) neurons in the substantia nigra (SNc) and dopamine transporter (DAT) in the striatum. Representative images illustrating TH^+ neurons in the SNc area (**A**). The number of DA neurons in the SNc was counted in each animal using unbiased stereoinvestigator system as described in "methods" section. The number of DA neurons was significantly higher in the SNc of the Control group (V + Sal) when compared to the MPTP group (V + MPTP). TQ treatment significantly rescued the DA neurons from the MPTP-induced neurodegeneration (**B**). Representative images showing the immunoreactivity of DAT in the striatum. The expression of dopamine nerve terminals was significantly reduced in the striatum of MPTP-injected mice as compared with that in the control (V + Sal) group. TQ treatment prior to MPTP shows significant attenuation of dopamine nerve terminals (**C**). DAT intensity was measured using NIH image and presented in the graph (**D**). Values are means ± SEM (n = 4–5 animals). ***, $p < 0.001$; *, $p < 0.05$.

treatment with TQ prior to MPTP injection prevented the MPTP-induced loss of DA neurons ($p < 0.05$) in the SNc and striatal DA fibers ($p < 0.05$), compared to the MPTP group animals. Moreover, TQ alone did not cause any deleterious changes on DA neurons in the SNc and striatum (Fig. 1). Therefore, this result suggests that TQ treatment provides neuroprotection against MPTP.

3.2. Effect of TQ on lipid peroxidation and GSH levels in the striatum

We investigated whether the neuroprotective effect of TQ against MPTP was mediated through its antioxidant and anti-inflammatory effect. As expected, mice administered with MPTP showed a significant ($p < 0.01$) increase in the lipid peroxidation product MDA compared to the control group. Concomitantly, MPTP administration caused a significant ($p < 0.001$) decrease in GSH levels when compared to the control group. Since TQ has antioxidant activity, we investigated whether it had a role in inhibiting MDA generation and normalizing GSH levels. Interestingly, we found that mice pre-treated with TQ prior to MPTP injection showed a significant ($p < 0.001$) reduction in MDA levels and improved GSH levels ($p < 0.01$) when compared to the MPTP group; however, mice treated with only TQ (i.e., TQ + Sal group) did not show significant alteration in the levels of MDA and GSH compared to control animals (Fig. 2C/D).

3.3. Effect of TQ on antioxidant enzyme activity in striatal tissues

We also measured the activity of antioxidant enzymes, SOD and CAT, which were found to be significantly decreased ($p < 0.001$) in MPTP-injected animals in comparison with control animals; however, treatment with TQ significantly increased ($p < 0.001$) the activity of SOD and CAT when compared to the MPTP control group. We did not observe any significant changes in the activity of CAT between controls and TQ alone treated animals (Fig. 2B). However, TQ alone treated animals showed a decrease in SOD levels when compared to the control group (Fig. 2A). The reason for the low SOD level in the TQ group is currently unknown; therefore, further study is necessary to elucidate its effect on SOD activity.

3.4. Effect of TQ on the induction of pro-inflammatory cytokines in the striatum

We also measured the concentration of pro-inflammatory cytokines IL-1β, IL-6, and TNF-α in the striatum to determine the role of neuroinflammation and its attenuation caused by TQ. MPTP administration induced a significant increase in the level of pro-inflammatory cytokines compared to the control group; however, TQ treatment significantly decreased the elevated level of these pro-inflammatory cytokines in MPTP-challenged animals (i.e., TQ + MPTP) when compared to the MPTP (i.e., V + MPTP) group. Mice treated only with TQ (i.e., TQ + Sal) did not show any increase in the levels of pro-inflammatory

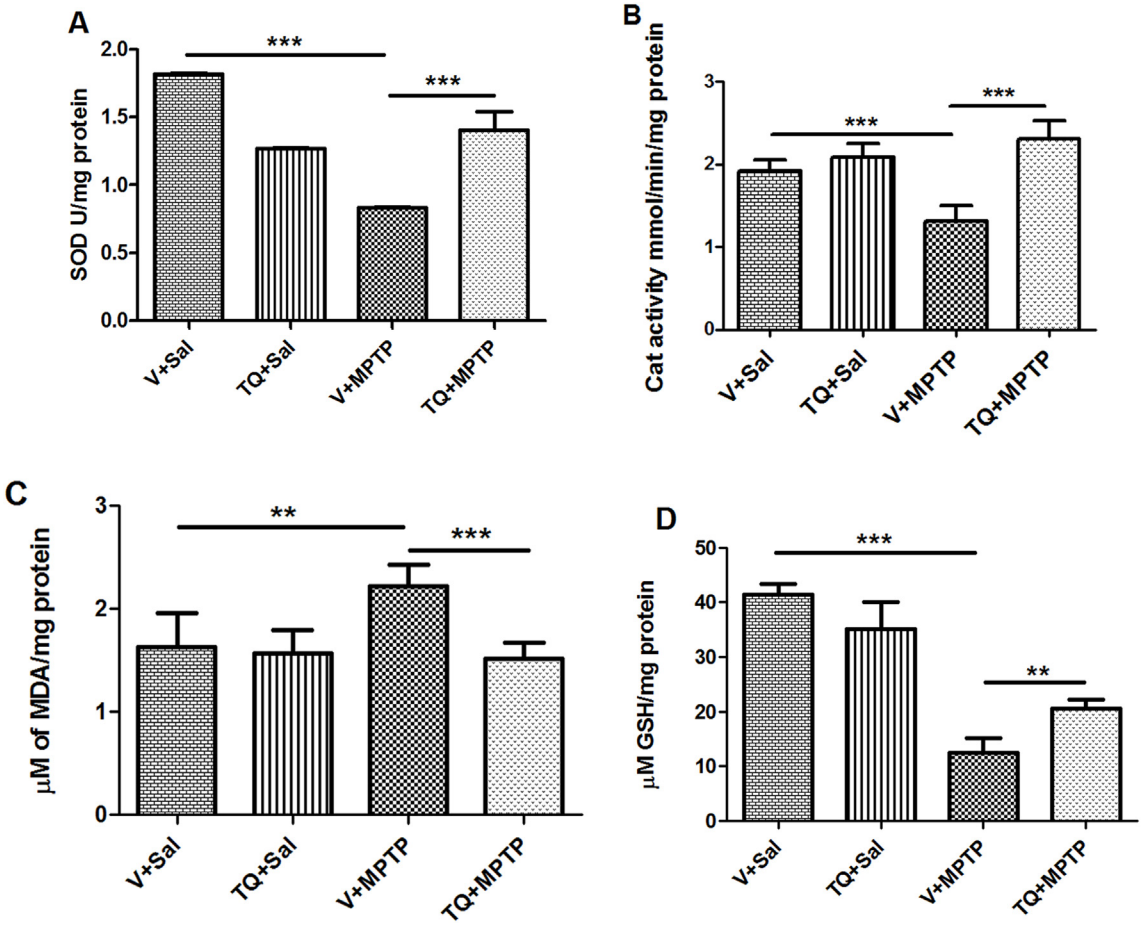

Fig. 2. Quantification of SOD, Catalase, MDA and GSH in the striatal tissue of different experimental groups. MPTP injections significantly decreases the activities of SOD (**A**) and Catalase (**B**). It also increases the lipid peroxidation product, malondialdehyde (MDA) (**C**) and decreases the total glutathione (GSH) (**D**) in the striatum of MPTP treated mice relative to control (V + Sal) group. Thymoquinone (TQ) treatment prior to MPTP significantly increases the activities of SOD and Catalase. It also decreases the level of MDA and increases the level of total GSH. Values are expressed as means ± SEM (n = 4–5). ***, $p < 0.001$; **, $p < 0.01$.

cytokines when compared to control group animals (Fig. 3).

3.5. Effect of TQ on inflammatory mediators: striatal COX-2 and iNOS expression

We further investigated the expression of COX-2 and iNOS using Western blots in the cytoplasmic fraction of striatal tissue lysates (Fig. 4). The expression level of COX-2 was increased in MPTP-challenged mice, compared to control mice (Fig. 4C/D); however, treatment with TQ in MPTP-challenged mice decreased the elevated level of COX-2 compared to the MPTP group (Fig. 4C/D). Similarly, we also observed an increase in iNOS expression in the MPTP-injected animals compared to the control animals (Fig. 4A/B). Alternatively, following treatment with TQ in MPTP-administered mice, a significant reduction in the level of iNOS was observed when compared to MPTP treated group (i.e., V + MPTP). TQ alone injected mice did not cause any alterations in the expression levels of COX-2 and iNOS (Fig. 4A/B).

3.6. TQ inhibited α-syn amyloid fibril formation

One of the pathological hallmarks of PD is the deposition of α-syn as Lewy bodies. It has been considered that α-syn plays a critical role in the development of PD; hence, we examined whether TQ has any effect in preventing fibril formation. α-syn at a concentration of 25 µM was incubated with continuous shaking for 9 days at 37 °C, and fibril formation was monitored by Th-S fluorescence assay at specific time points. In the experimental group, α-syn was incubated with TQ at molar ratios of 1:4, 1:2, and 1:1 (α-syn:TQ).

Interestingly, we found that TQ inhibited α-syn aggregation, as indicated by the reduced Th-S fluorescence (Fig. 5A). More specifically, at a concentration of 100 µM, TQ exhibited a significant inhibitory effect, which was prominent from the fifth day of incubation. After 9 days of incubation (Fig. 5B), TQ at 100 µM abolished almost 64% of the α-syn fibrillation, while at 50 µM it inhibited fibrillation by almost 28%. At lower concentrations (i.e., 25 µM), TQ also induced inhibition of α-syn fibrillation by approximately 16% after 9 days of incubation. Moreover, the IC_{50} of TQ was determined to be 80 µM (Fig. 5B). These results indicate that TQ inhibited fibril formation in a dose-dependent manner.

To confirm the above findings, further tests were carried out, such as immunoblotting and electron microscopy. Samples of α-syn were incubated alone or in the presence of TQ at different molar ratios for 9 days and were used in immunoblotting. The radiographs (Fig. 5C) show clear inhibition of the high molecular weight aggregates in a 4:1 sample comparing α-syn sample aged alone, which supports our results. Transmission electron microscopy images of α-syn aged in the presence of TQ showed different morphological features, unlike the dense meshes of long fibrils formed by α-syn aged alone (Fig. 5D), which also explain why a reduced Th-S signal was previously obtained.

3.7. TQ disaggregates preformed α-syn amyloid fibrils

As TQ was shown to be an effective inhibitor of α-syn fibrillation, we examined whether it was possible for TQ to reverse the fibrillation process. Hence, 25 µM of preformed α-syn fibrils were incubated at

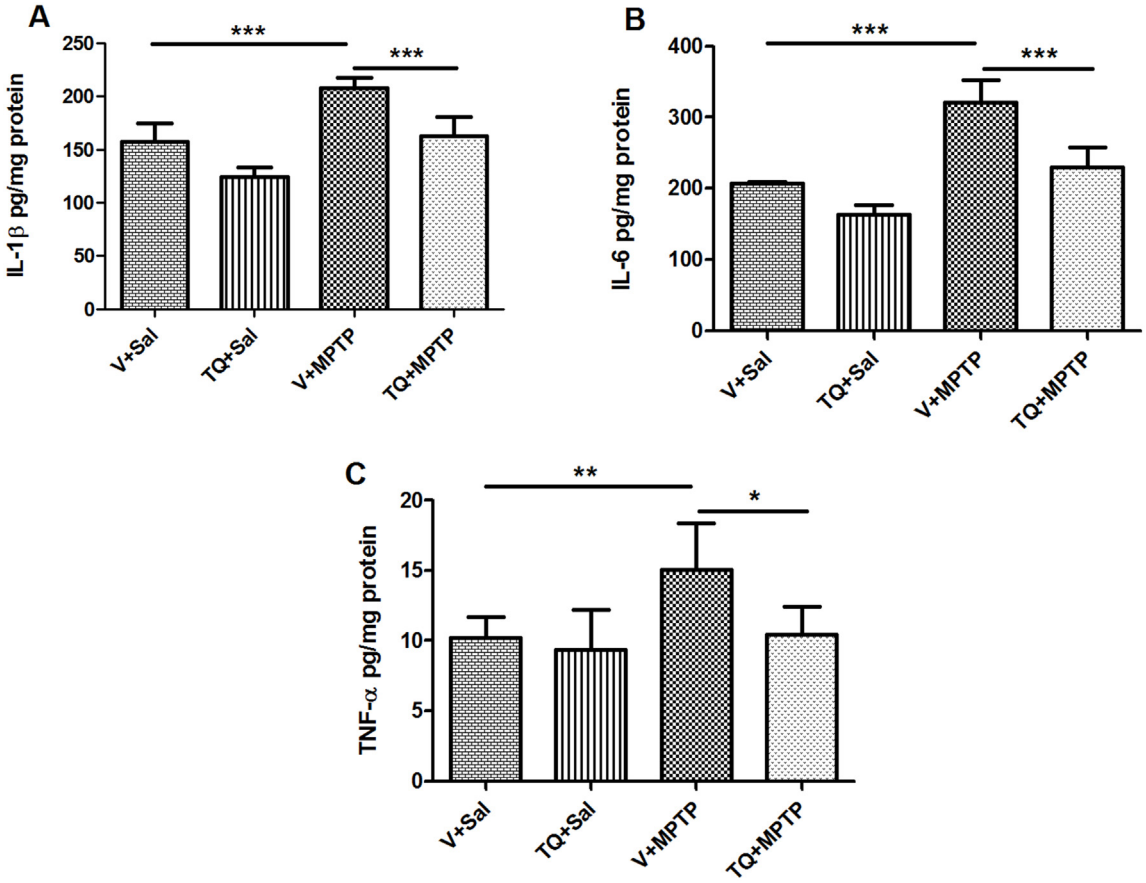

Fig. 3. Quantification of IL-1β, IL-6, and TNF-α in the striatal tissue. Enzyme-linked immunosorbent assay (ELISA) was carried out to quantify IL-1β, IL-6, and TNF-α in the striatal tissue of different experimental groups. MPTP treatment significantly increases the level of IL-1β, IL-6 and TNF-α. TQ pretreatment prior to MPTP injection significantly reduced the level of IL-1β (**A**), IL-6 (**B**), and TNF-α (**C**) when compared to MPTP treated animals. Values are expressed as means ± SEM (n = 4–5). ***, $p < 0.001$; **, $p < 0.01$; *, $p < 0.05$.

37 °C for 48 h in the presence of TQ at TQ:α-syn molar ratios of 6:1, 4:1, and 1:1. Fibril content formation was then estimated by measuring the intensity of Th-S fluorescence emission at different time points (0, 2, 4, 6, 24, and 48 h) (Fig. 6A). At 0 h, Th-S counts were approximately 2000 for α-syn incubated alone or in the presence of TQ, whereas α-syn fibrils that were incubated alone continued to aggregate further over time, as indicated by the increase in Th-S counts (Fig. 6A). α-syn fibrils incubated in the presence of TQ significantly disaggregated after 48 h, as seen as a decrease in Th-S counts. The disaggregation occurred in a dose-dependent fashion that reached its highest levels after 48 h with a 6:1 M ratio concentration (Fig. 6A).

3.8. TQ interfered with the seeding of α-syn monomers

Mechanistically, amyloid fibril formation takes place in a three step process, according to a nucleation-dependent polymerization model (Jarrett and Lansbury, 1992). It starts with "nucleation" or the "lag time" phase, where soluble species nucleate to form oligomeric species, which then polymerize in a phase called "polymerization" or the "growth" phase to produce the final insoluble fibrils ("equilibrium" phase). This process was accelerated by the presence of small aggregates or seeds that bypassed the nucleation phase of amyloid fibril formation *in vitro* and *in vivo* through a process called seeding. Our results determined that TQ interfered with the formation of α-syn fibrils (Fig. 5A/B) and disaggregated preformed α-syn fibrils (Fig. 6A). Therefore, we sought to determine whether this compound would affect the seeding of α-syn aggregation.

As expected, the addition of the short fibrillar seeds accelerated the fibrillation process of α-syn monomers (Fig. 6B). Remarkably, TQ at concentrations of 10 and 50 μM significantly inhibited the seeding process at each time point, as indicated by the low Th-S counts, suggesting that TQ interferes with the α-syn seeding process. We also tested whether the α-syn aggregates formed in the presence of TQ were resistant to PK digestion. Interestingly, we observed that aged α-syn, in the presence of TQ, was easily digested by PK treatment and behaved similar to monomeric α-syn (Fig. 6C).

3.9. The effect of TQ on α-syn-induced cytotoxicity

SH-SY5Y cells were treated either with α-syn aged alone or with TQ for 9 days at three different concentrations: 1.25, 2.5, and 5 μM. The viability of the cells was determined by the MTT assay. Prior to any experiments, the effect of TQ on cell viability was assessed, employing the same non-toxic TQ concentrations that were later employed for the experiments with aged α-syn solutions (data not shown).

Aged α-syn inhibited the reduction of MTT in a dose-dependent manner (Fig. 6D), given that MTT reduction is directly proportional to the number of surviving cells. It became apparent that the higher the concentration of aged α-syn, the lower the number of cells that survived (Fig. 6D). However, aged α-syn solutions in the presence of TQ (4:1 and 2:1 ratios) were less toxic to the cells, as indicated by the increased MTT reduction (Fig. 6D), which is directly proportional to the number of living cells. Moreover, 5 μM of α-syn aged alone induced the reduction of viable cells by almost 75% (25% survival), whereas in the presence of TQ (4:1 ratio), the survival of the cells improved dramatically (65% survival). Interestingly, at molar ratios of 4:1, TQ was proved to be a

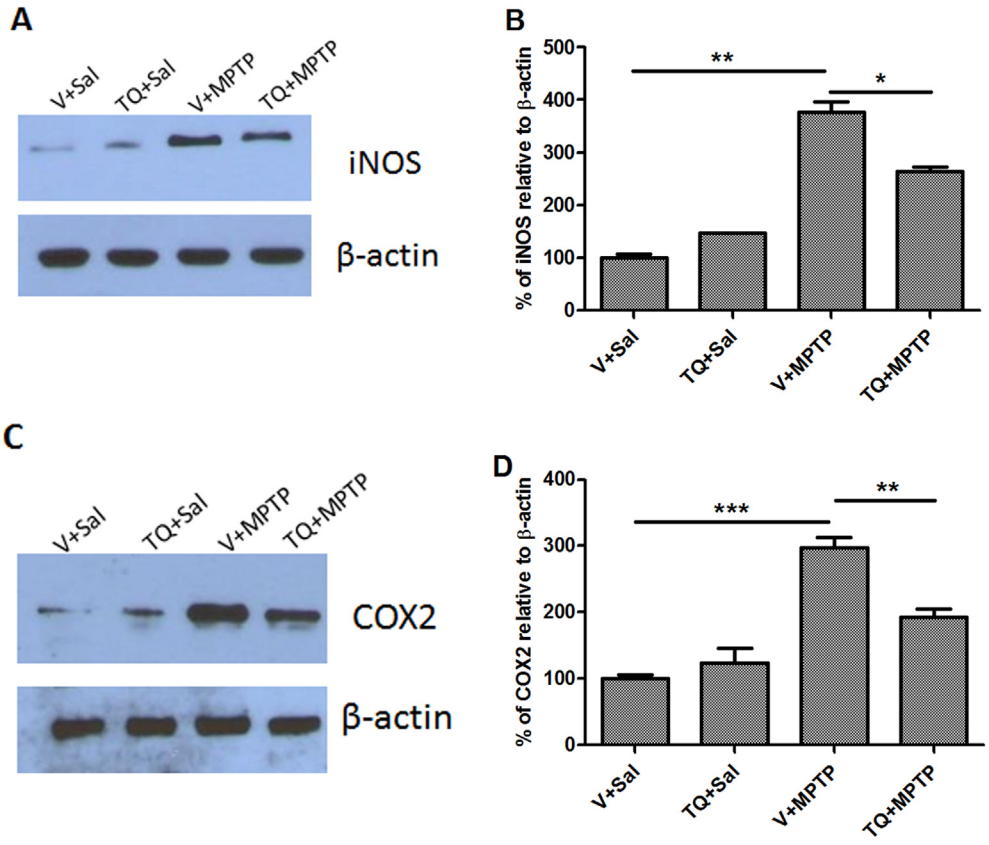

Fig. 4. Western blot analysis to examine the expression of inducible nitric oxide synthase (iNOS) and cyclooxygenase-2 (COX-2) in the striatal tissue. A significant increase in iNOS was observed in the MPTP group relative to the control (V + Sal) group. Thymoquinone (TQ) treatment followed by MPTP injection significantly decreased the expression of iNOS relative to the MPTP group (**A/B**). Similarly, COX2 expression was increased significantly in MPTP group relative to the control (V + Sal) group. TQ treatment notably decreased the COX2 expression relative to the MPTP group (**C/D**). Values are expressed as percentage of means ± SEM relative to CONT group. ***, $p < 0.001$; **, $p < 0.01$; *, $p < 0.05$.

good inhibitor of fibril formation, as indicated by the reduction in Th-S counts (Fig. 5A). These findings are in agreement with the Th-S fluorescence measurements (Fig. 5A) and Western blot analyses (Fig. 5C), which indicated the inhibition of α-syn aggregation using TQ (4:1 M ratio).

4. Discussion

PD is the second most common neurodegenerative disorder after Alzheimer's disease; however, its cause is still unknown. A large amount of literature suggests that mitochondrial defects, oxidative stress, neuroinflammation, and unfolded protein stress are critical in the development of PD. There are two major pathological hallmarks observed in PD patient brains: selective degeneration of dopaminergic neurons in the SNc and accumulation of intracellular protein aggregates in the surviving neurons known as Lewy bodies. PD is a progressive neurodegenerative disorder, in which current medication cannot halt its development. The drugs available to combat the PD only can alleviate the clinical symptoms; however, over time they cause many side effects such levodopa-induced dyskinesia, wearing-off or off-period dyskinesia, and diphasic dyskinesia (Pandey and Srivanitchapoom, 2017). It has been a great challenge for researchers to develop new drugs that can halt dopaminergic neuronal death and improve the motor and non-motor symptoms simultaneously. Thus, in the current study, we have explored the possibility of whether compounds available in nature with medicinal properties can cease dopaminergic neuronal death in a preclinical model of PD.

Nigella sativa, known as black seed, was traditionally used to treat neurodegenerative, coronary artery, respiratory, and urinary tract diseases. TQ is a naturally occurring active compound abundant in black seed. It has been credited with many medicinal properties such as anti-inflammatory, antioxidative, anticancer, antibacterial, antimutagenic and antigenotoxic activities (Su et al., 2016; Badary et al., 2007; Velagapudi et al., 2017a, 2017b; Ozer et al., 2017; Elsherbiny et al., 2017; Shao et al., 2016; Mostofa et al., 2017; Barkat et al., 2018; Alobaedi et al., 2017; Rifaioglu et al., 2013; Inci et al., 2013; Dehghani et al., 2015). As previously described, oxidative stress, neuroinflammation, mitochondrial dysfunction, and misfolded protein stress are thought to play a critical role to PD development. Since TQ possesses anti-inflammatory and antioxidative properties, in the current study, we tested the neuroprotective efficacy of TQ on an MPTP animal model of PD. MPTP is a lipophilic compound that can cross the blood brain barrier and accumulate in DA neurons in the SNc through a DA transporter after being converted to MPP + by glial cells. MPP + can displace DA from the synaptic vesicles, as well as block Complex I of the mitochondrial electron transport system. As a result, it generates reactive oxygen species (ROS) and depletes ATP, which ultimately leads to DA neuron loss in the SNc of the brain. Due to the selective damage caused by MPTP in SNc neurons, it has been used to generate a preclinical model of PD, which can also summarize the clinical features of PD in primate and rodent models. Thus, in the current study, we selected an MPTP model of PD to test the efficacy of TQ. Previously it has been demonstrated that TQ can prevent dopaminergic neurodegeneration in 6-OHDA (Sedaghat et al., 2014) and rotenone models of PD (Radad et al., 2009; Ebrahimi et al., 2017); however, such models have limitations. Moreover, TQ studies using 6-OHDA or rotenone models were not comprehensive (Sedaghat et al., 2014; Radad et al., 2009; Ebrahimi et al., 2017). It has been demonstrated that TQ can prevent behavioral defects that occur in the presence of rotenone (Ebrahimi et al., 2017). Furthermore, TQ can alter mitochondrial sensor proteins such as parkin and dynamin related protein 1, which are induced by rotenone. However, although rotenone can be used to induce models of PD, there are notable limitations, as it can target any neuron, including DA neurons, and cause mitochondrial dysfunction.

MPTP has been shown to lead to selective dopaminergic lesions in the SNc by increasing oxidative stress and altering the antioxidant capacities of SOD, catalase, and GSH. Similar to earlier reports, we also observed that MPTP at 25 mg/kg *b. wt.* can significantly reduce SOD,

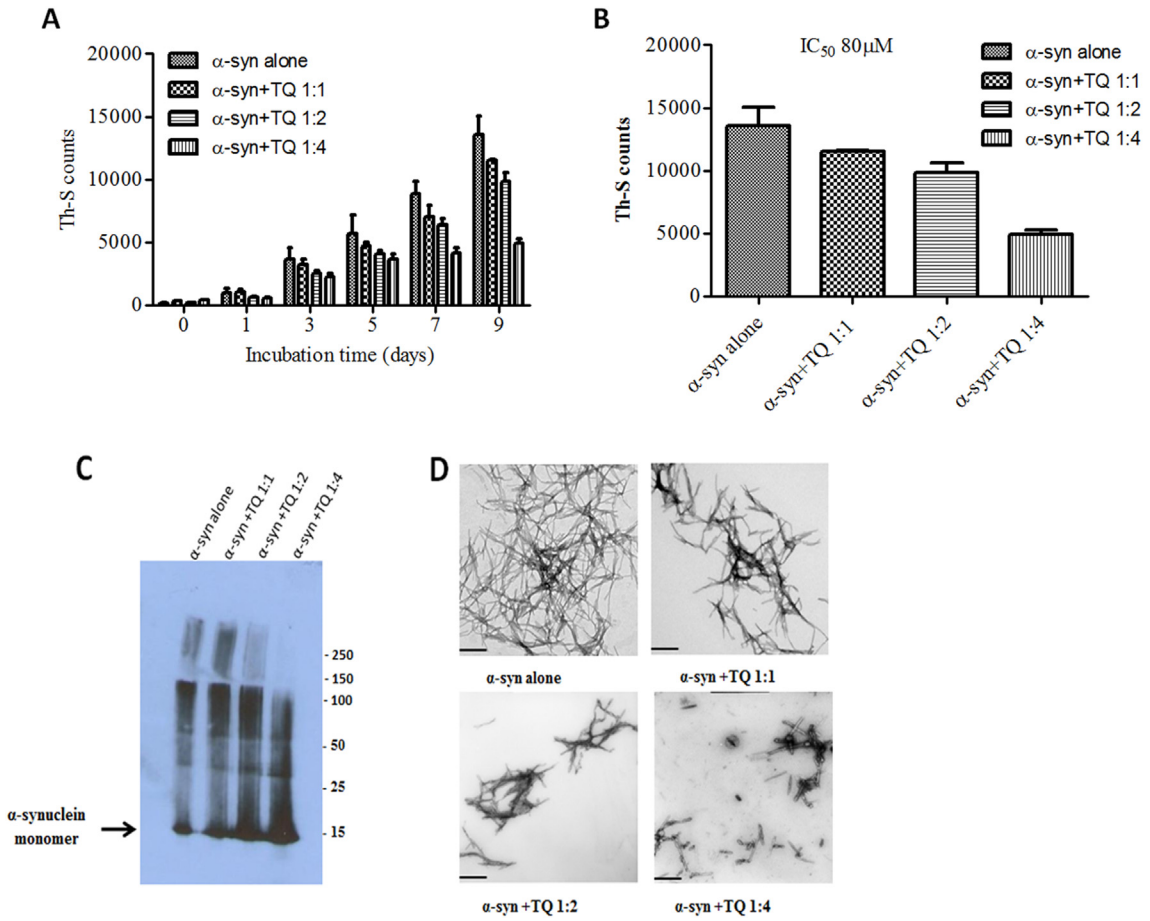

Fig. 5. TQ inhibits α-syn fibrillation in a dose-dependent manner. Samples of α-syn (25 μM) were incubated alone or in the presence of TQ (molar ration of TQ: α-syn 4:1, 2:1, 1:1) for 9 days with continuous shaking at 37 °C. Fibril formation was estimated by Th-S fluorescence assay. The assay was performed in triplicate average of triplicate measurement ± standard deviation (**A**). Fibril formation was estimated by Th-S fluorescence at day 9 and presented (**B**). Immunoblot analysis of the effect of TQ on α-syn oligomerization. Fresh α-syn alone or in the presence of TQ at molar ratios of α-syn: TQ 1:1, 1:21 and 1:4 incubated for 9 days with continuous shaking at 37 °C were separated by electrophoresis in a15% SDS-PAGE gel. Lane 1: α-syn only; lane 2: α-syn: TQ 1:1; lane3: α-syn: TQ 1:2; lane 4 α-syn: TQ 1:4 M ratios of α-syn and TQ (**C**). Electron microscopy images of negatively stained samples of α-syn (25 μM) incubated for 9 days alone or in the presence of TQ (molar ratio of α-syn: TQ: 1:1, 1:2:1, 1:4, (**D**). *Scale bar* 500 nm.

catalase, and GSH levels, while also increasing the lipid peroxidation product MDA. We found that pretreatment with TQ significantly normalized the enzyme activities of SOD and catalase, two important endogenous antioxidant enzymes. TQ also modulated GSH levels, suggesting its antioxidant properties. The downstream consequence of ROS generation is the further generation of lipid peroxidation product (MDA) due to the oxidation of lipids, which results from MPTP intoxication. We also observed an increased level of MDA in the striatum of MPTP injected animals, whereas TQ administration prior to MPTP prevented MDA generation; this is consistent with previous results citing the antioxidant properties of TQ.

Neuroinflammation is critical in neurodegenerative disorders, including PD (Hassanzadeh and Rahimmi, 2018; Gelders et al., 2018; Skaper et al., 2018). We observed that MPTP exposure leads to a significant increase in inflammatory markers such as IL-1, IL-6, and TNF-α. It has been previously determined that MPTP causes neuroinflammation (Lofrumento et al., 2011; Vroon et al., 2007); therefore, we have sought to examine whether TQ has any role in preventing such effect. We found that TQ inhibited the increase of neuroinflammatory cytokines that are observed in MPTP intoxication. We also measured mediators of inflammation, COX-2 and iNOS, by performing Western blotting. We observed that TQ administration caused a significant attenuation of COX-2 and iNOS activation. It is noteworthy that iNOS knockout mice are resistant to MPTP, suggesting that activation of iNOS is important in this model (Liberatore et al., 1999). The presence of reactive microglia in the SNc of primates years after MPTP administration has also been observed (McGeer et al., 2003).

One of the key pathological features of PD is the degeneration of dopaminergic neurons in the SNc. MPTP is a neurotoxic compound that has been shown to cause DA neuron loss in multiple organisms such as humans, mice, and monkeys (Langston et al., 1984; Lofrumento et al., 2011; Vroon et al., 2007; Liberatore et al., 1999; McGeer et al., 2003). Thus, it has been considered a clinically relevant model for testing potential drugs. MPTP exposure in mice causes significant degeneration of DA neurons in the SNc, as counted by unbiased stereology using the StereoInvestigator system. SNc neurons project their nerve terminals to the striatum and any degeneration in the SNc will cause DAT retraction. In the present study, MPTP-treated animals clearly showed a decrease in DAT, suggesting the loss of DA neurons in the SNc. TQ treatment before MPTP intoxication rescued DA neurons in the SNc, as well as a DAT loss in the striatum.

One of the key pathological hallmarks of PD is the abnormal deposition of intracellular protein aggregates to the surviving neurons, known as Lewy bodies. A major component of Lewy bodies is α-syn, a 140-amino acid protein whose function is currently unknown. The formation of fibrillar protein aggregates, often called amyloid fibrils, is a central feature of many diseases (Eisenberg and Jucker, 2012), including systemic amyloidosis (Wechalekar et al., 2016), Alzheimer's disease (Ow and Dunstan, 2014), and PD (Goedert et al., 2015). The mechanism of protein fibril formation dictates the rate of protein fibril

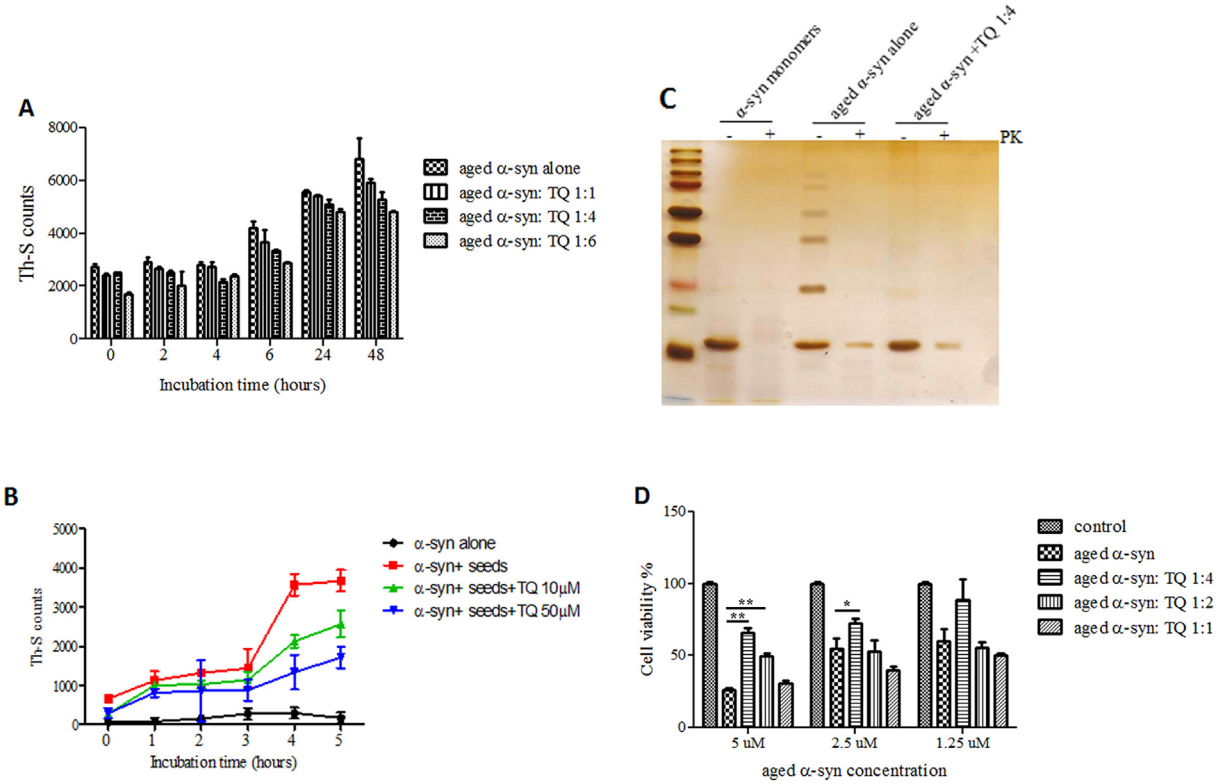

Fig. 6. TQ disaggregates preformed α-syn fibrils in a dose-dependent manner and prevents cell death. Samples of aggregated α-syn were incubated for 48 h at 37 °C in the absence or presence of various concentrations of TQ (aged α-syn: TQ: 1:6, 1:4, 1:1). The fibril content was then measured by the Th-S binding assay (**A**). The assays were performed in triplicate (average of triplicate measurements ± standard deviations). Monomeric α-syn (100 μM) containing α-syn seeds (2 μM) incubated alone or in the presence of 10 or 50 μM TQ for 5 h with continuous shaking at 37 °C. The extent of fibrillation was estimated by Th-S binding assay. The assays were performed in triplicate (average of triplicate measurements ± standard deviations) (**B**). Silver staining for 15% SDS gel of α-syn monomers, α-syn aged alone or in the presence of TQ at molar ratio 1:4 (α-syn: TQ: 1:4) for 9 days and then digested with PK (**C**). The disaggregation of preformed α-syn fibrils by TQ generated species that were less toxic to the cells. The viability of SH-SY5Y human neuroblastoma cells was assessed by the MTT assay. The results are expressed as percentages of the control average (i.e. untreated cells). The α-syn species generated by 72 h incubation of preformed α-syn fibrils in the presence or absence of TQ were added to the cells 48 h prior to MTT addition (average of 3 wells ± SD (**D**). Statistical analysis was performed using two tailed unpaired *t*-test, **, $p < 0.01$; *, $p < 0.05$).

formation, the type of intermediates that exist during this process (which may be more toxic than the final products), and how long these intermediates exist in the cells. These factors are crucial as they are likely to dictate disease onset, progression, and toxicity. *In vitro* studies of protein fibrillation mechanisms are therefore important for understanding diseases associated with protein fibril formation (Chiti and Dobson et al., 2017). Unfortunately, protein fibril formation mechanisms can be complicated, making it difficult to correlate experimental observations with specific mechanisms. α-syn is naturally present in its unfolded form; it can form an alpha helix structure once it binds to the membrane through a complex transition from a monomer to an oligomer and finally to fibril formation. It has been demonstrated that the oligomeric species of this protein can be toxic. Previously, it has been shown that TQ attenuates the toxic effect of glutamate through inhibiting amyloidogenic and apoptotic pathways, as well as that nanoemulsion fractions containing TQ decrease Aβ40 and Aβ42 levels by modulating amyloid precursor protein and inhibiting beta-secretase 1 (Ismail et al., 2017). TQ also prevents cultured cerebellar granule neurons from Aβ neurotoxicity (Ismail et al., 2013) and can prevent Aβ mitochondrial dysfunction and oxidative stress (Khan et al., 2012). Moreover, previous reports have found that TQ protects the cultured hippocampal and human-induced pluripotent stem cell-derived neurons against α-syn-induced synaptic damage (Alhebshi et al., 2014). These studies suggest that TQ also inhibits synuclein-mediated toxicity.

In the current study, we further explored whether TQ had a role in preventing α-syn fibril formation. Interestingly, we found that TQ significantly prevented the generation of preformed fibrils from monomeric α-syn when incubated together. TQ inhibited fibril formation in a dose-dependent fashion, as shown in Fig. 5 A-D. TQ also interfered with the seeding of monomeric synuclein accelerated by the addition of α-syn preformed fibril. Moreover, TQ were able to disintegrate preformed fibrils into monomeric α-syn; however, this mechanism is unclear. To determine the role of TQ in preventing preformed fibril-induced toxicity, we used a cell line that had been previously used (Paleologou et al., 2008; Ardah et al., 2014a). We found that TQ prevented SH-SY5Y cell lines from preformed fibril-induced toxicity in a dose dependent manner. Thus, based on our findings, we speculate that the neuroprotective effects of TQ are mediated by its antioxidant and anti-inflammatory actions and partly by its ability to inhibit the aggregation of α-syn. However, it is noteworthy that DA neurons of α-syn knockout mice are resistant to MPTP. Additionally, we found that silencing synuclein in the mouse brain provides neuroprotection against MPTP. Our results indirectly suggest that TQ-mediated neuroprotection against MPTP may serve as an aid against α-syn aggregation. Future studies will be required to extend the present study and examine the *in vivo* model system.

5. Concluding remarks

PD is the most common movement disorder mostly affecting the population aged 60 years or older. Currently, there are no preventive drugs available that can halt the degeneration of the subset of neurons that produce DA. The only treatment available is DA replacement therapy, which can only alleviate the clinical symptoms. In the present

study, we tested the beneficial effect of TQ, a compound that is abundant in black seed. We observed that TQ pretreatment, prior to MPTP insult, can induce a neuroprotective effect by enhancing antioxidant capacity and inhibiting neuroinflammation. We also found that TQ delayed α-syn aggregation and seeding, thereby preventing cellular toxicity in an *in vitro* cellular model. Thus, further studies are needed to examine its *in vivo* role in α-syn-induced toxicity and α-syn propagation.

Funding

This work was supported by a research grant (grant code: 31M332) from the College of Medicine and Health Sciences, United Arab Emirates University to MEH.

Conflicts of interest

There are no patents, products in development, or marketed products to declare. This study was supported by grant from the College of Medicine & Health Sciences, UAE University, UAE. The funders had no role in study design, data collection and analysis, decision to publish, or preparation of the manuscript.

Ethical approval

All procedures performed in studies involving animals were in accordance with the ethical standards of the Animal Research Ethics Committee, United Arab Emirates University, UAE.

Acknowledgments

We thank Mahmoud Hag Ali, the Animal Research Facility controller for his help with animal care and welfare.

References

AbuKhader, M.M., 2013. Thymoquinone in the clinical treatment of cancer: fact or fiction. Phcog. Rev. 7 (14), 117–120.

Ahmad, A., Husain, A., Mujeeb, M., Khan, S.A., Najmi, A.K., Siddique, N.A., Damanhouri, Z.A., Anwar, F., 2013 May. A review on therapeutic potential of Nigella sativa: a miracle herb. Asian Pac. J. Trop. Biomed. 3 (5), 337–352. https://doi.org/10.1016/S2221-1691(13)60075-1.

Alhebshi, A., Odawara, A., Gotoh, M., Suzuki, I., 2014. Thymoquinone protects cultured hippocampal and human induced pluripotent stem cells-derived neurons against α-synuclein-induced synapse damage. Neurosci. Lett. 570, 126–131.

Alobaedi, O.H., Talib, W.H., Basheti, I.A., 2017 Apr. Antitumor effect of thymoquinone combined with resveratrol on mice transplanted with breast cancer. Asian Pac. J. Trop. Med. 10 (4), 400–408. https://doi.org/10.1016/j.apjtm.2017.03.026. Epub 2017 Apr 7.

Angeles, D.C., Ho, P., Dymock, B.W., Lim, K.L., Zhou, Z.D., Tan, E.K., 2016 Mar 2. Antioxidants inhibit neuronal toxicity in Parkinson's disease-linked LRRK2. Ann. Clin. Transl. Neurol. 3 (4), 288–294. https://doi.org/10.1002/acn3.282.

Ardah, M.T., Paleologou, K.E., Lv, G., Menon, S.A., Abul Khair, S.B., Lu, J.H., et al., 2014a. Ginsenoside Rb1 inhibits fibrillation and toxicity of alpha-synuclein and disaggregates preformed fibrils. Neurobiol. Dis. 74C, 89–101.

Ardah, M.T., Paleologou, K.E., Lv, G., Abul Khair, S.B., Kazim, A.S., Minhas, S.T., et al., 2014b. Structure activity relationship of phenolic acid inhibitors of α-synuclein fibril formation and toxicity. Front. Aging Neurosci. 6, 197.

Badary, O.A., Abd-Ellah, M.F., El-Mahdy, M.A., Salama, S.A., Hamada, F.M., 2007 Jan. Food Chem Toxicol. Anticlastogenic activity of thymoquinone against benzo(a) pyrene in mice. 45 (1), 88–92 Epub 2006 Aug 30.

Barkat, M.A., Harshita, Ahmad, J., Khan, M.A., Beg, S., Ahmad, F.J., 2018. Insights into the targeting potential of thymoquinone for therapeutic intervention against triple-negative breast cancer. Curr. Drug Targets 19 (1), 70–80. https://doi.org/10.2174/1389450118666170612095959.

Beal, M.F., 2003 Jun. Mitochondria, oxidative damage, and inflammation in Parkinson's disease. Ann. N. Y. Acad. Sci. 991, 120–131.

Casey, C., Caroline, S., Leonard, P., 2012 May. Disruption of protein quality control in Parkinson's disease. Cold Spring Harb. Perspect. Med. 2 (5), a009423. https://doi.org/10.1101/cshperspect.a009423.

Chiti, F., Dobson, C.M., 2017 Jun 20. Protein misfolding, amyloid formation, and human disease: a summary of progress over the last decade. Annu. Rev. Biochem. 86, 27–68. https://doi.org/10.1146/annurev-biochem-061516-045115. Epub 2017 May 12.

Conway, K.A., Lee, S.J., Rochet, J.C., Ding, T.T., Williamson, R.E., Lansbury Jr., P.T., 2000. Acceleration of oligomerization, not fibrillization, is a shared property of both alpha-synuclein mutations linked to early-onset Parkinson's disease: implications for pathogenesis and therapy. Proc. Natl. Acad. Sci. U.S.A. 97, 571–576.

Dehghani, H., Hashemi, M., Entezari, M., Mohsenifar, A., 2015. The comparison of anticancer activity of thymoquinone and nanothymoquinone on human breast adenocarcinoma. Iran. J. Pharm. Res. (IJPR) 14 (2), 539–546 Spring;.

Ebrahimi, S.S., Oryan, S., Izadpanah, E., Hassanzadeh, K., 2017 Jul 5. Thymoquinone exerts neuroprotective effect in animal model of Parkinson's disease. Toxicol. Lett. 276, 108–114. https://doi.org/10.1016/j.toxlet.2017.05.018. Epub 2017 May 17.

El-Agnaf, O.M., Walsh, D.M., Allsop, D., 2003. Soluble oligomers for the diagnosis of neurodegenerative diseases. Lancet Neurol. 2, 461–462.

Elmaci, I., Altinoz, M.A., 2016 Oct. Thymoquinone: an edible redox-active quinone for the pharmacotherapy of neurodegenerative conditions and glial brain tumors. A short review. Biomed. Pharmacother. 83, 635–640.

Elsherbiny, N.M., Maysarah, N.M., El-Sherbiny, M., Al-Gayyar, M.M., 2017 Jul 1. Renal protective effects of thymoquinone against sodium nitrite-induced chronic toxicity in rats: impact on inflammation and apoptosis. Life Sci. 180, 1–8. https://doi.org/10.1016/j.lfs.2017.05.005. Epub 2017 May 8.

Eisenberg, D., Jucker, M., 2012 Mar 16. The Amyloid State of Proteins in Human diseases.Cell, vol. 148. pp. 1188–1203. https://doi.org/10.1016/j.cell.2012.02.022. 6.

Gelders, G., Baekelandt, V., Van der Perren, A., 2018 Apr 16. Linking neuroinflammation and neurodegeneration in Parkinson's disease. J Immunol Res. 2018, 4784268. https://doi.org/10.1155/2018/4784268. eCollection 2018.

Goedert, M., 2015 Aug 7. NEURODEGENERATION. Alzheimer's and Parkinson's diseases: the prion concept in relation to assembled Aβ, tau, and α-synuclein. Science 349 (6248), 1255555. https://doi.org/10.1126/science.1255555.

Gore, P.R., Prajapati, C.P., Mahajan, U.B., Goyal, S.N., Belemkar, S., Ojha, S., Patil, C.R., 2016. Protective effect of thymoquinone against cyclophosphamide-induced hemorrhagic cystitis through inhibiting DNA damage and upregulation of Nrf2 expression. Int. J. Biol. Sci. 12 (8), 944–953.

Hald, A., Lotharius, J., 2005 Jun. Oxidative stress and inflammation in Parkinson's disease: is there a causal link? Exp. Neurol. 193 (2), 279–290.

Hamdy, N.M., Taha, R.A., 2009. Effects of Nigella sativa oil and thymoquinone on oxidative stress and neuropathy in streptozotocin-induced diabetic rats. Pharmacology 84 (3), 127–134.

Haque, M.E., Mount, M.P., Safarpour, F., Abdel-Messih, E., Callaghan, S., Mazerolle, C., Kitada, T., Slack, R.S., Wallace, V., Shen, J., Anisman, H., Park, D.S., 2012 Jun 29. Inactivation of PINK1 gene *in vivo* sensitizes dopamine producing neurons to 1-methyl-4-phenyl -1,2,3,6-tetrahydropyridine (MPTP) and can be rescued by autosomal recessive PD genes, Parkin or DJ-1. J. Biol. Chem. 287 (27), 23162–23170. https://doi.org/10.1074/jbc.M112.346437. Epub 2012 Apr 17.

Hassanzadeh, K., Rahimmi, A., 2018 Jan. Oxidative stress and neuroinflammation in the story of Parkinson's disease: could targeting these pathways write a good ending? J. Cell. Physiol. 234 (1), 23–32. https://doi.org/10.1002/jcp.26865. Epub 2018 Aug 4.

He, X.J., Uchida, K., Megumi, C., Tsuge, N., Nakayama, H., 2015 Oct. Dietary curcumin supplementation attenuates 1-methyl-4-phenyl-1,2,3,6-tetrahydropyridine(MPTP) neurotoxicity in C57BL mice. J. Toxicol. Pathol. 28 (4), 197–206.

Inci, M., Davarci, M., Inci, M., Motor, S., Yalcinkaya, F.R., Nacar, E., Aydin, M., Sefil, N.K., Zararsiz, I., 2013 Apr. Anti-inflammatory and antioxidant activity of thymoquinone in a rat model of acute bacterial prostatitis. Hum. Exp. Toxicol. 32 (4), 354–361. https://doi.org/10.1177/0960327112455068. Epub 2012 Aug 7.

Ismail, N., Ismail, M., Mazlan, M., Latiff, L.A., Imam, M.U., Iqbal, S., Azmi, N.H., Ghafar, S.A., Chan, K.W., 2013 Nov. Thymoquinone prevents β-amyloid neurotoxicity in primary cultured cerebellar granule neurons. Cell. Mol. Neurobiol. 33 (8), 1159–1169. https://doi.org/10.1007/s10571-013-9982-z. Epub 2013 Oct 8.

Ismail, N., Ismail, M., Azmi, N.H., Bakar, M.F.A., Yida, Z., Abdullah, M.A., Basri, H., 2017 Nov. Biomed Pharmacother. Thymoquinone-rich fraction nanoemulsion (TQRFNE) decreases Aβ40 and Aβ42 levels by modulating APP processing, up-regulating IDE and LRP1, and down-regulating BACE1 and RAGE in response to high fat/cholesterol diet-induced rats. 95, 780–788. https://doi.org/10.1016/j.biopha.2017.08.074. Epub 2017 Sep. 8.

Jarrett, J.T., Lansbury, P.T., 1992. Amyloid fibril formation requires a chemically discriminating nucleation event: studies of an amyloidogenic sequence from the bacterial protein OsmB. Biochemistry 31 (49), 12345–12352.

Khan, A., Vaibhav, K., Javed, H., Khan, M.M., Tabassum, R., Ahmed, M.E., Srivastava, P., Khuwaja, G., Islam, F., Siddiqui, M.S., Safhi, M.M., Islam, F., 2012 Oct. Attenuation of Aβ-induced neurotoxicity by thymoquinone via inhibition of mitochondrial dysfunction and oxidative stress. Mol. Cell. Biochem. 369 (1–2), 55–65. https://doi.org/10.1007/s11010-012-1368-x. Epub 2012 Jul 1.

Langston, J.W., Langston, E.B., Irwin, I., 1984. MPTP-induced parkinsonism in human and non-human primates–clinical and experimental aspects. Acta Neurol. Scand. Suppl. 100, 49–54.

Liberatore, G.T., Jackson-Lewis, V., Vukosavic, S., Mandir, A.S., Vila, M., McAuliffe, W.G., Dawson, V.L., Dawson, T.M., Przedborski, S., 1999 Dec. Inducible nitric oxide synthase stimulates dopaminergic neurodegeneration in the MPTP model of Parkinson disease. Nat. Med. 5 (12), 1403–1409.

Lofrumento, D.D., Saponaro, C., Cianciulli, A., De Nuccio, F., Mitolo, V., Nicolardi, G., Panaro, M.A., 2011. MPTP-induced neuroinflammation increases the expression of pro-inflammatory cytokines and their receptors in mouse brain. Neuroimmunomodulation 18 (2), 79–88. https://doi.org/10.1159/000320027. Epub 2010 Oct 13.

Luk, K.C., Kehm, V.M., Zhang, B., O'Brien, P., Trojanowski, J.Q., Lee, V.M., 2012. Intracerebral inoculation of pathological α-synuclein initiates a rapidly progressive neurodegenerative α-synucleinopathy in mice. J. Exp. Med. 209 (5), 975–986.

Luk, K.C., Kehm, V., Carroll, J., Zhang, B., O'Brien, P., Trojanowski, J.Q., Lee, V.M., 2012. Pathological α-synuclein transmission initiates Parkinson-like neurodegeneration in

nontransgenic mice. Science 338 (6109), 949–953.
McGeer, P.L., Schwab, C., Parent, A., Doudet, D., 2003 Nov. Presence of reactive microglia in monkey substantia nigra years after 1-methyl-4-phenyl-1,2,3,6-tetrahydropyridine administration. Ann. Neurol. 54 (5), 599–604.
Mostofa, A.G.M., Hossain, M.K., Basak, D., Bin Sayeed, M.S., 2017 Jun 12. Thymoquinone as a potential adjuvant therapy for cancer treatment: evidence from preclinical studies. Front. Pharmacol. 8, 295. https://doi.org/10.3389/fphar.2017.00295. eCollection 2017.
Ojha, S., Javed, H., Azimullah, S., Abul Khair, S.B., Haque, M.E., 2016 Feb. Glycyrrhizic acid attenuates neuroinflammation and oxidative stress in rotenone model of Parkinson's disease. Neurotox. Res. 29 (2), 275–287. https://doi.org/10.1007/s12640-015-9579-z.
Ow, S.Y., Dunstan, D.E., 2014 Oct. A brief overview of amyloids and Alzheimer's disease. Protein Sci. 23 (10), 1315–1331. https://doi.org/10.1002/pro.2524. Epub 2014 Jul 30.
Ozer, E.K., Goktas, M.T., Toker, A., Pehlivan, S., Bariskaner, H., Ugurluoglu, C., Iskit, A.B., 2017 Aug. Thymoquinone protects against the sepsis induced mortality, mesenteric hypoperfusion, aortic dysfunction and multiple organ damage in rats. Pharmacol. Rep. 69 (4), 683–690. https://doi.org/10.1016/j.pharep.2017.02.021. Epub 2017 Mar 24.
Paleologou, K.E., Schmid, A.W., Rospigliosi, C.C., Kim, H.Y., Lamberto, G.R., Fredenburg, R.A., et al., 2008. Phosphorylation at Ser-129 but not the phosphomimics S129E/D inhibits the fibrillation of alpha-synuclein. J. Biol. Chem. 283 (24), 16895–16905.
Pandey, S., Srivanitchapoom, P., 2017 Jul-Sep -Sep. Levodopa-induced dyskinesia: clinical features, pathophysiology, and medical management. Ann. Indian Acad. Neurol. 20 (3), 190–198. https://doi.org/10.4103/aian.AIAN_239_17.
Radad, K., Moldzio, R., Taha, M., Rausch, W.D., 2009 May. Thymoquinone protects dopaminergic neurons against MPP+ and rotenone. Phytother Res. 23 (5), 696–700. https://doi.org/10.1002/ptr.2708.
Radad, K.S., Al-Shraim, M.M., Moustafa, M.F., Rausch, W.D., 2015 Jan. Neuroprotective role of thymoquinone against 1-methyl-4-phenylpyridinium-induced dopaminergic cell death in primary mesencephalic cell culture. Neurosciences 20 (1), 10–16.
Rifaioglu, M.M., Nacar, A., Yuksel, R., Yonden, Z., Karcioglu, M., Zorba, O.U., Davarci, I., Sefil, N.K., 2013. Antioxidative and anti-inflammatory effect of thymoquinone in an acute Pseudomonas prostatitis rat model. Urol. Int. 91 (4), 474–481. https://doi.org/10.1159/000351261. Epub 2013 Sep 3.
Rocha, E.M., De Miranda, B., Sanders, L.H., 2018 Jan. Alpha-synuclein: pathology, mitochondrial dysfunction and neuroinflammation in Parkinson's disease. Neurobiol. Dis. 109 (Pt B), 249–257. https://doi.org/10.1016/j.nbd.2017.04.004. Epub 2017 Apr 8.
Sanders, L.H., Greenamyre, J.T., 2013 Sep. Oxidative damage to macromolecules in human Parkinson disease and the rotenone model. Free Radic. Biol. Med. 62, 111–120.
Sedaghat, R., Roghani, M., Khalili, M., 2014 Winter. Neuroprotective effect of thymoquinone, the nigella sativa bioactive compound, in 6-hydroxydopamine-induced hemi-parkinsonian rat model. Iran. J. Pharm. Res. (IJPR) 13 (1), 227–234.
Shao, Y., Feng, Y., Xie, Y., Luo, Q., Chen, L., Li, B., Chen, Y., 2016 Dec. Protective effects of thymoquinone against convulsant activity induced by lithium-pilocarpine in a model of status epilepticus. Neurochem. Res. 41 (12), 3399–3406 Epub 2016 Oct 18.
Skaper, S.D., Facci, L., Zusso, M., Giusti, P., 2018 Mar 21. An inflammation-centric view of neurological disease: beyond the neuron. Front. Cell. Neurosci. 12, 72. https://doi.org/10.3389/fncel.2018.00072. eCollection 2018.
Su, X., Ren, Y., Yu, N., Kong, L., Kang, J., 2016 Sep. Thymoquinone inhibits inflammation, neoangiogenesis and vascular remodeling in asthma mice. Int. Immunopharmacol. 38, 70–80. https://doi.org/10.1016/j.intimp.2016.05.018. Epub 2016 May 27.
Taka, E., Mazzio, E.A., Goodman, C.B., Redmon, N., Flores-Rozas, H., Reams, R., Darling-Reed, S., Soliman, K.F., 2015 Sep 15. Anti-inflammatory effects of thymoquinone in activated BV-2 microglial cells. J. Neuroimmunol. 286, 5–12.
Tinakoua, A., Bouabid, S., Faggiani, E., De Deurwaerdère, P., Lakhdar-Ghazal, N., Benazzouz, A., 2015 Dec 17. The impact of combined administration of paraquat and maneb on motor and non-motor functions in the rat. Neuroscience 311, 118–129.
Uversky, V.N., Lee, H.J., Li, J., Fink, A.L., Lee, S.J., 2001. Stabilization of partially folded conformation during alpha-synuclein oligomerization in both purified and cytosolic preparations. J. Biol. Chem. 276, 43495–43498.
Velagapudi, R., Kumar, A., Bhatia, H.S., El-Bakoush, A., Lepiarz, I., Fiebich, B.L., Olajide, O.A., 2017 Jula. Inhibition of neuroinflammation by thymoquinone requires activation of Nrf2/ARE signalling. Int. Immunopharmacol. 48, 17–29. https://doi.org/10.1016/j.intimp.2017.04.018. Epub 2017 May 3.
Velagapudi, R., El-Bakoush, A., Lepiarz, I., Ogunrinade, F., Olajide, O.A., 2017 Novb. AMPK and SIRT1 activation contribute to inhibition of neuroinflammation by thymoquinone in BV2 microglia. Mol. Cell. Biochem. 435 (1–2), 149–162. https://doi.org/10.1007/s11010-017-3064-3. Epub 2017 May 27.
Vroon, A., Drukarch, B., Bol, J.G., Cras, P., Brevé, J.J., Allan, S.M., Relton, J.K., Hoogland, P.V., Van Dam, A.M., 2007 Aug. Neuroinflammation in Parkinson's patients and MPTP-treated mice is not restricted to the nigrostriatal system: microgliosis and differential expression of interleukin-1 receptors in the olfactory bulb. Exp. Gerontol. 42 (8), 762–771 Epub 2007 Apr 29.
Wechalekar, A.D., Gillmore, J.D., Hawkins, P.N., 2016 Jun 25. Systemic amyloidosis. Lancet 387 (10038), 2641–2654. https://doi.org/10.1016/S0140-6736(15)01274-X. Epub 2015 Dec 21.
Winner, B., Jappelli, R., Maji, S.K., Desplats, P.A., Boyer, L., Aigner, S., et al., 2011. In vivo demonstration that alpha-synuclein oligomers are toxic. Proc. Natl. Acad. Sci. U.S.A. 108, 4194–4419.